Supplementary material

S.1) Filter measurements uncertainty

As mentioned in Sect. 2, undenuded filter measurements, like those performed during the campaign, are subject to artefacts, related to volatilisation of semi-volatile material (SVM, mostly organic compounds and ammonium nitrate) (Pang et al., 2002) and/or adsorption of gaseous species. Additionally, artefacts strongly depend on the type of filter, and notably on its ability to retain gaseous compounds (among which HNO_3 and NH_3) (Yu-Hsiang et al., 1997; and references therein). In southern California, Hering and Cass (1999) have estimated that 28% on average of the particulate nitrate is lost when using Teflon filters as compared to denuded nylon ones, with a large monthly variability. During a filter intercomparison (including Teflon filters) over 10 months at 19 sites with mean temperatures ranging from -20 to 30°C (i.e. roughly comparable to temperatures in Paris over the year), Keck et al. (2005) have shown that negative artefacts on ammonium nitrate (and chloride) are negligible below 0°C for Teflon filters. Above that threshold temperature, losses increase with temperature, to approximately 20-30% at 10°C, around 40% at 20°C, until complete loss above 25°C. Conversely, the low ability to retain gases on Teflon filters (contrary to cellulose acetate-nitrate filters for instance) may lead to lower positive artefacts in ambient conditions with significant gaseous HNO_3 or NH_3 concentrations.

For both nitrate and OA, intercomparison exercises have shown reasonable agreement with a particle-into-liquid-sampler (PILS) coupled with ion chromatography (IC) and an OCEC Sunset field instrument respectively (Bressi et al., 2012), but during a wintertime period with potentially low evaporation. These artefacts are likely to increase in spring and summer with changing ambient conditions. Hering and Cass (1999) have shown that the seasonal variation of undenuded Teflon filter losses approximately ranges from 10% in winter to 80% in summer.

Thanks to the available TEOM-FDMS measurements at the PAR station, it is possible to investigate the semi-volatile contribution to $PM_{2.5}$. This instrument operates at 30°C, and provides a reference $PM_{2.5}$ measurement, including both non-volatile and semi-volatile parts, as well as the split between both. Gravimetric and TEOM-FDMS measurements are compared in Fig. S1. The correlation between both measurements is strong (R=0.97). The semi-volatile part (at 30°C) measured by the TEOM-FDMS, ranging from 1 to 14 $\mu g.m^{-3}$, is stronger in winter and spring, due to higher temperature discrepancies between the instrument and ambient conditions as well as higher particulate concentrations. This semi-volatile matter is likely essentially composed of ammonium nitrate and organic matter (Huffmann et al., 2009). Actually, its correlation with nitrate appears

significantly stronger than with OM (0.88 against 0.53), which may indicate a larger contribution of this former compound.

Most of the time, gravimetric measurements underestimate the $PM_{2.5}$ concentration, with maximum relative biases reaching around -50%. Strongest negative relative discrepancies occur in early autumn and spring. Additionally, positive biases (probably by adsorption) are observed in August. If they reach +50%, these latter biases are not so problematic as they occur when concentrations are very low, and should thus not influence considerably the budget results. The gravimetric measurement usually gives higher concentrations than the reference non-volatile one, probably because it operates at lower temperature (ambient room temperature compared to 30°C) and is thus expected to evaporate less material.

Let us assume that the difference between the corrected TEOM-FDMS $PM_{2.5}$ concentration and the gravimetric measurement is essentially composed of ammonium nitrate and OM. It corresponds to the net artefact. One can compute its relative contribution to the total of ammonium nitrate plus OM corrected by this loss:

$$\Delta = \frac{PM_{ref} - PM_{grav}}{OM + NH_4NO_3 + PM_{ref} - PM_{grav}} \quad (15)$$

Figure S2 shows the evolution of this relative error over the year. Maximum delta values reach 60% in autumn and summer, while they range between 10 and 40% during winter and spring. Highest (negative) values occur in August when concentrations are low, and are thus not likely to influence considerably budget results. From this figure, one can roughly estimate an OM plus ammonium nitrate loss around -30% in winter and -50% in summer (except August).

S.2) PM emissions speciation

The Table S1 gives the $PM_{2.5}$ speciation used in the ESMERALDA simulation platform, for the large and the two other refined domains. Speciation in the Paris region is deduced from the local detailed emission inventory (at a SNAP sector level of 3) and speciation factors from the literature.

S.3) Evidence of woodburning local impact at the RNE station

Daily levoglucosan measurements are available at PAR, RNE and RUS stations. Their concentrations are represented in Fig. S3, as well as temperature and OM rural levels. The figure shows strong OM discrepancies between the RNE station on one side, and the two other rural ones on the other side (up

to a factor of five on specific days). They are not systematic, but appear occasionally from October to May. Such large discrepancies are also clearly observed for levoglucosan concentrations, which indicate that these differences are probably related to local woodburning pollution. The contribution of road transport is likely to be minor, since no similar trend is observed for EC concentrations during these events. Even during north-easterly wind regimes, these large OM (and levoglucosan) amounts at the RNE station are not advected toward Paris (PAR concentrations below RNE ones), which suggests a local origin. These OM data thus need to be invalidated, as well as the PM one.

However, considering the importance of NE sector, both in terms of frequency (31%, see Sect. 5.2) and PM imports, a criteria has been defined to discriminate such local pollution events from real imports at the RNE stations, in order to retain as many data as possible. Despite a large distance between stations (around 100 km), rural OM concentrations appear quite homogeneous. The median values of RNE/RUS, RNE/RNW and RUS/RNW ratios are 1.3, 1.3 and 1.0, respectively. We thus set at 30% the maximum relative discrepancy on OM concentration between RNE station and the two other rural ones, above which RNE data (OM and $PM_{2.5}$) is invalidated and replaced by mean data from RUS and/or RNW stations, depending on their availability. Results are illustrated in Fig. S4, where the correction of red points leads to green ones.

The choice of such a low threshold allows minimizing the risk of taking into account non-representative OM imports in the Paris budget. It implies a large recurrence of RNE data invalidation, 210 days out of 361. But actually, the procedure is here applied to all data and not only data associated to north-east origin (i.e. used to compute the advected contribution). The number of corrected points taken into account is thus lower. Sensitivity tests on this criterion show a satisfactory robustness of average (monthly, annual) results (monthly contributions do not change more than ±3% with criteria values in the 20-40% range).

S.4) Primary organic aerosol volatility

As primary organic aerosol (POA) is considered as non-volatile in the CHIMERE model, it is interesting to evaluate how strong the effect of its unaccounted volatility can be.

Let us consider an emission of POA. Given the semi-volatile nature of organic matter, this POA can be considered as semi-volatile OM (SVOM). Following Robinson et al. (2007), we also need to take into account intermediate-volatility OM (IVOM), estimated at 1.5*SVOM. For convenience, this total amount is denominated as SVOM (thus equal to 2.5*POA). As this SVOM includes a large number of species of various volatility, one can group them into 9 bins of volatility , $\{C_i^*\}_{i=(1;9)}$ with

respect to their reference saturation concentration at a given temperature of 298 K (Donahue et al., 2006):

$$\left\{C_i^*\right\} = \{0.01,0.1,1,10,100,1000,10000,100000\}\ \mu g.m^{-3} \quad (16)$$

The lumped species aggregating all the SVOM emitted in the volatility bin i is defined as $SVOM_i$, and its concentration as C_i. $\{C_i\}_{i=(1;9)}$ is assumed to follow the distribution illustrated by the bars height in Fig. S4, based on Robinson et al. (2007). At a given temperature, the partitioning theory describes the fraction f_i of the $SVOM_i$ species that would be present in the particulate phase through the following equation (Donahue et al., 2006):

$$f_i = \frac{1}{1+\frac{C_i^*}{C_{OA}}} \text{ with } C_{OA} = \sum_{i=1}^{9} f_i C_i \text{ the condensed-phase OA mass concentration.} \quad (17)$$

From this, it is now possible to compute the total fraction of emissions that stays in the particulate phase, depending on the temperature and the C_{OA} concentration. A change on C_{OA} and/or temperature (modifying C_i^* through Clausius-Clapeyron law) modifies the partitioning between both phases. Given an OA concentration and a temperature, it is thus possible to derive the amount of initial POA emissions that is likely to volatilize just after emission. The example given in Fig. S5 shows that, at a temperature of 298 K and an OA concentration of 10 $\mu g.m^{-3}$, only 26% of the traditional POA emissions stay in the particulate phase.

A similar exercise is performed for each day during the whole PARTICULES period, on the basis of the OA concentrations observed at the PAR site and the temperature measured in the city (MONTSOURIS station). Results are shown in Fig. S6. The part of volatilized POA emissions turns out to be very large, with values ranging from 40 to 80%. The consideration of POA volatility appears to be crucial in summer where most of emissions are volatilized (up to 4-5 time lower). While values are lower in winter, particularly during episodes, they remain significant.

S.5) Meteorology errors and impact on thermodynamic equilibria

As previously mentioned, thermodynamics of secondary inorganic salts (and water) are handled in CHIMERE using a tabulated version of the ISORROPIA module (Bessagnet et al., 2004). The amount of particulate ammonium nitrate depends on the total amounts in both gaseous and condensed phases of each compound of the system (sulfate plus sulfuric acid, nitrate plus nitric acid, ammonium plus ammonia) and on meteorological conditions (temperature, RH). We investigate here the

influence of meteorological errors on the thermodynamic equilibria, with a focus on nitrates. As described in Sect. 5.1, over the whole year, simulated temperature and RH in Paris show negative (-1°C) and positive biases (+3.1% RH), respectively. During specific episodes (cold or heat waves), errors can be much larger. This is likely to shift the equilibria towards the particulate phase, and we intend here to quantify the possible overestimation of particulate nitrate, based on the ISORROPIA table.

Let us consider over the Paris hourly temperature, RH and concentrations of each compound simulated by the model. By assuming for simplification that equilibrium is instantaneously achieved, one can compute with the ISORROPIA table the nitrate partition between gaseous and condensed phases. The same can be done with the temperature and the RH observed at MONTSOURIS station in Paris. Results are shown in Fig. S7.

As expected, the correction of temperature and RH reduces the amount of nitrate in the condensed phase. On average, the nitrate overestimation induced by these meteorological errors remains quite low, with absolute and relative bias around 0.3 $\mu g.m^{-3}$ and 10%, respectively. However, during summer, when most of nitrate is volatilized due to higher temperatures, biases can reach a factor of two. More precisely, discrepancies significantly depend on the distance between the simulated RH and the deliquesence RH (DRH, around 62% for ammonium nitrate). Therefore, meteorological errors in Paris are not likely to affect so much the overall nitrate budget simulated by CHIMERE since they are far lower than measurement uncertainties on average.

However, they can be more critical during specific meteorological events, during which errors on temperature and RH are likely to increase. Such an event occurs in the second half of June, where the heat wave in most of Europe is simulated with a cold bias (between -1 to more than -3°C), as shown over the continental domain on Fig. S8 (meteorological observations at all worldwide synoptic stations available from the British Atmospheric Data Center (BADC) (UK meteorological office)).

The previous analysis is applied to meteorological errors in Paris. Similar errors at the regional scale are not likely to influence directly the amount of particulate nitrate advected towards the city, since equilibrium is expected to be fast enough (compared to transportation time), depending mainly on the local meteorological conditions. However, an overestimation of the condensed phase far from Paris decreases gaseous nitric acid (HNO_3) concentrations and dry deposition, faster than particulate nitrate, along the transport and thus increases the available reservoir (nitric acid plus nitrate), which may finally be a factor of nitrate overestimation (in the case of negative temperature biases).

Table S1: $PM_{2.5}$ speciation (in %) for different SNAP sectors.

		Continental			Paris region		
SNAP sector		EC	OC	MPM*	EC	OC	MPM*
1	Public electricity and other energy transformation	10	10	80	45.1	38.3	16.6
2	Small combustion plants	15.8	54.7	29.5	15	54.2	30.8
3	Industrial combustion and processes with contact	25	30	45	32.9	32.4	34.6
4	Industrial process emission	0	10	90	0	14.1	85.9
5	Fossil fuel production	24.3	40	35.7	-**	-**	-**
6	Solvent and product use	24	40	36	0	0	100
7	Road transport	54.3	45.7	0	61.3	37	1.7
8	Other (non-road) transport and mobile machinery	54.7	20	25.3	59.4	32.8	7.8
9	Waste disposal	24.7	40	35.3	1.7	7.7	90.6
10	Agriculture	24	40	36	4.8	3.3	91.9

* MPM: Mineral particulate matter.

** No emissions in Paris region for this SNAP 5.

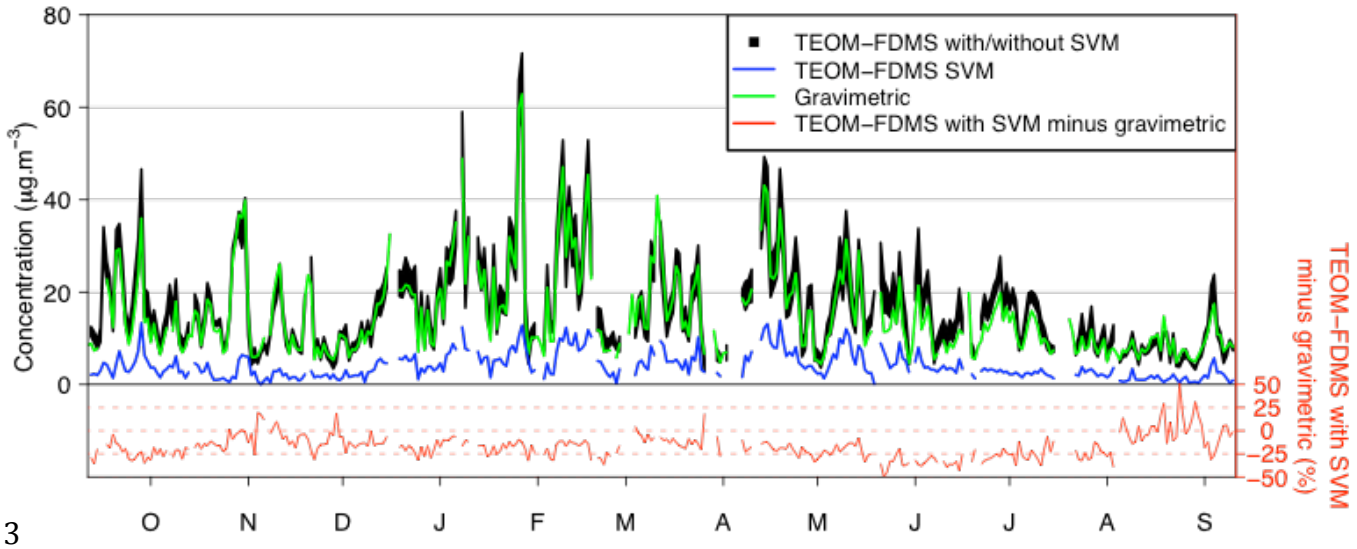

Figure S1: $PM_{2.5}$ concentrations ($\mu g.m^{-3}$) at the PAR site. $PM_{2.5}$ semi-volatile material (SVM) concentration is represented within the $PM_{2.5}$ total concentration in black (i.e. bottom and top of black surface correspond to TEOM-FDMS without and with SVM, respectively), and alone in blue. The gravimetric $PM_{2.5}$ at 20% RH is plotted in green. The relative discrepancy between reference (TEOM-FDMS with SVM) and gravimetric $PM_{2.5}$ (%) is plotted in red.

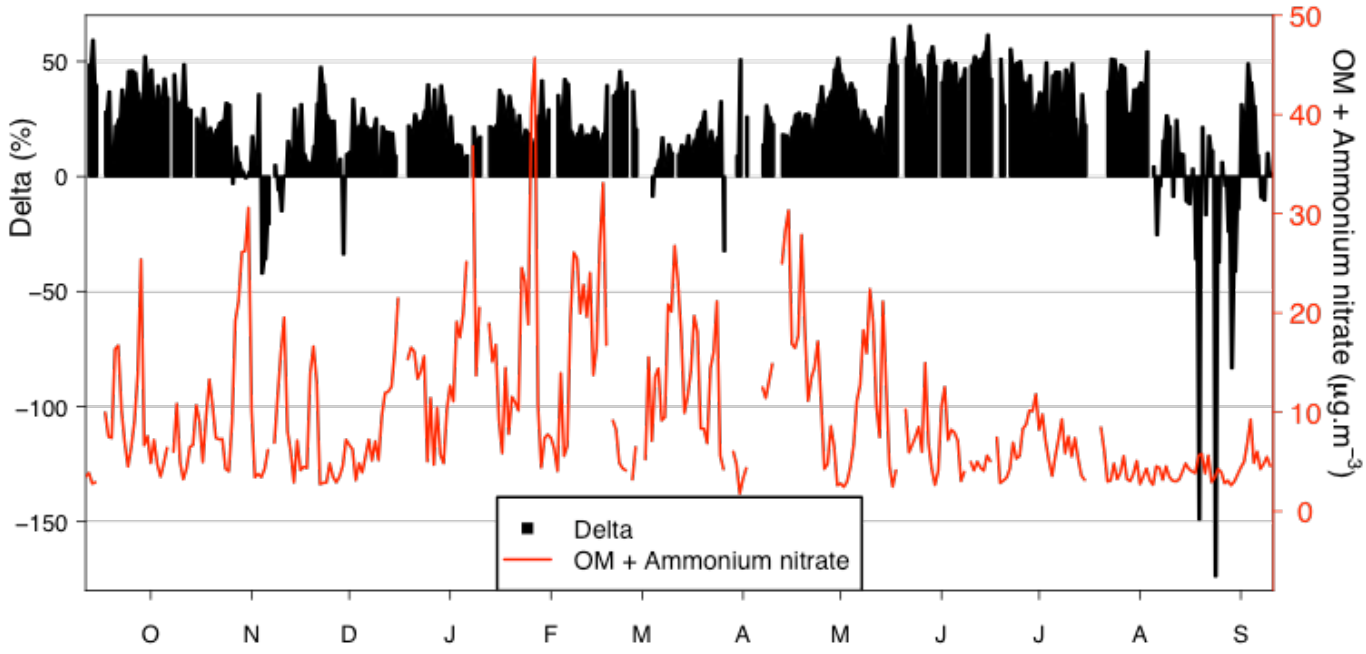

Figure S2: Delta time series (in black) (see text for explanations) and OM plus ammonium nitrate concentration (in red).

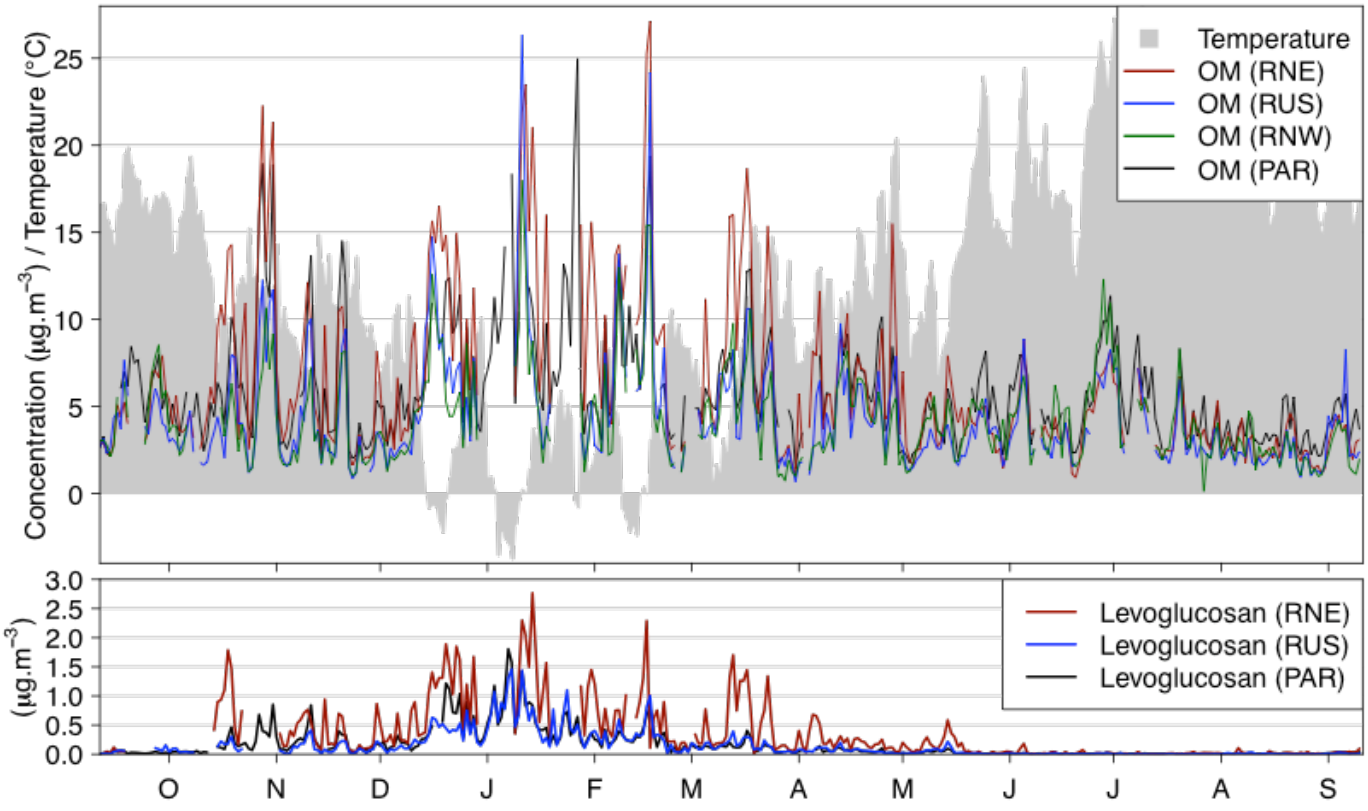

Figure S3: Temperature at MONTSOURIS station and OM concentration at rural stations (top panel), and levoglucosan concentrations (bottom panel).

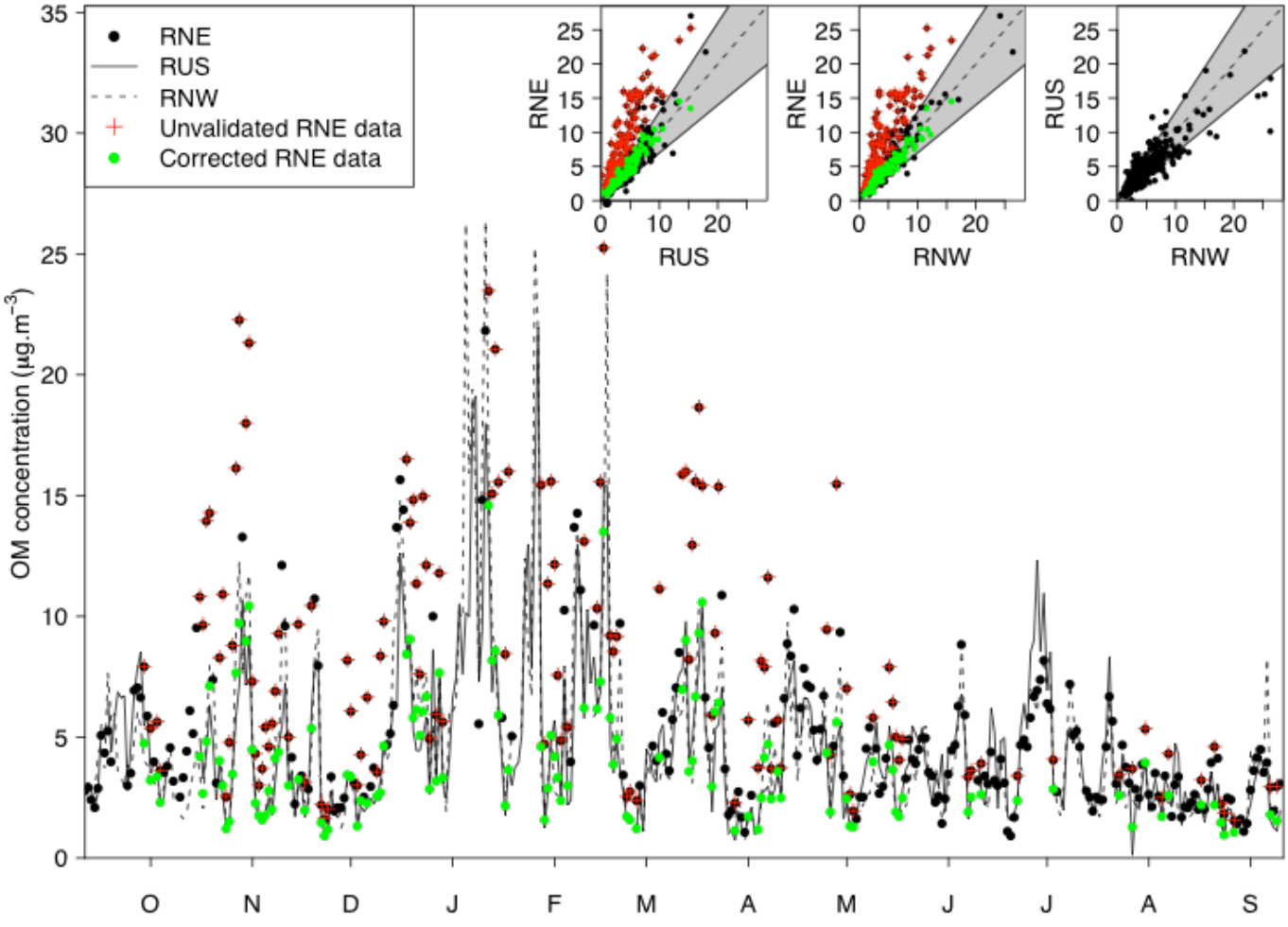

Figure S4 : OM concentration at all rural background stations (RNE, RUS, RNW) before correction (in black), unvalidated and corrected RNE points (in red and green, respectively). At the top of the figure, associated OM concentrations scatter plots of rural stations pairs (y=x in dotted line, and y=x±30%x in grey).

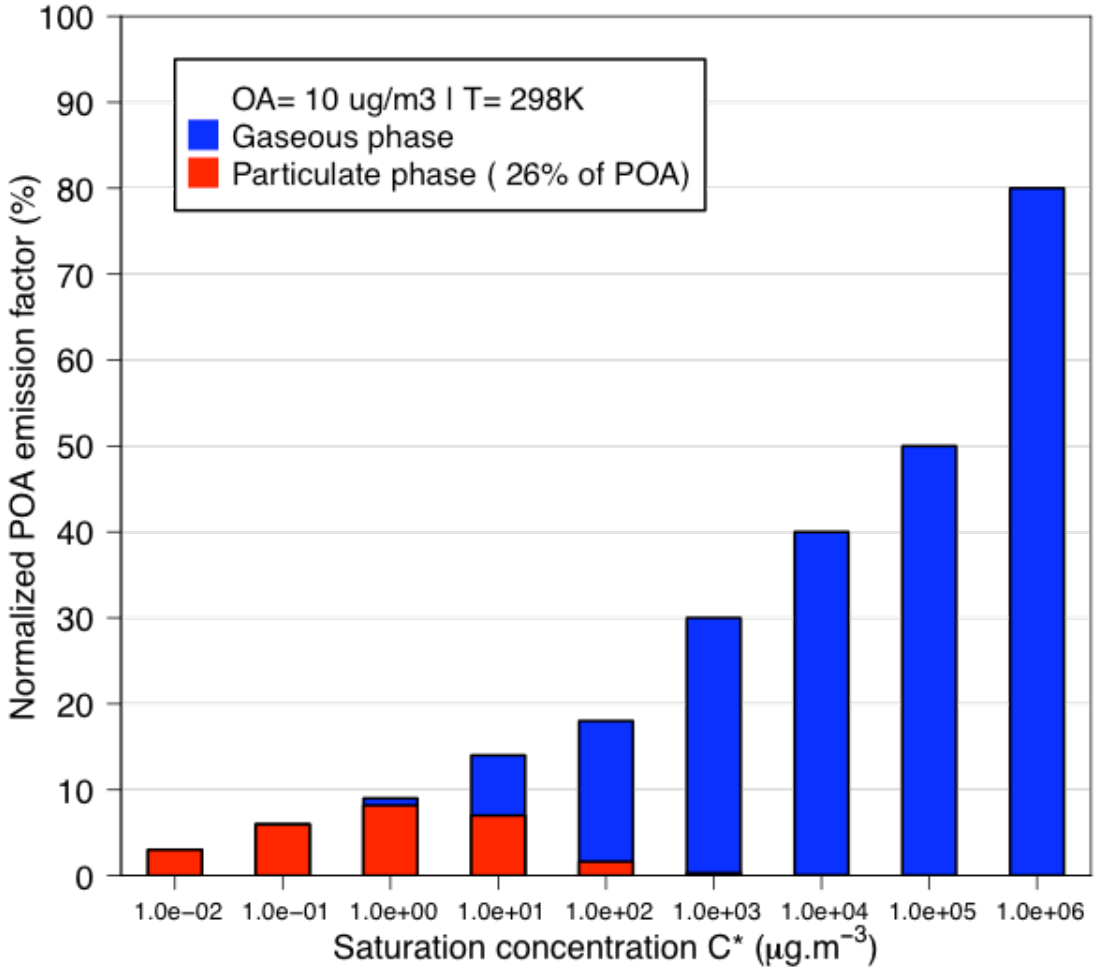

Figure S5: Distribution of SVOM emissions per volatility class normalized by POA emissions (i.e. total area equal to 250% of POA), with partitioning between particulate (in red, equal to 26% of POA) and gaseous (in blue) phases at a temperature of 298K and an OA concentration of 10 µg.m^{-3}.

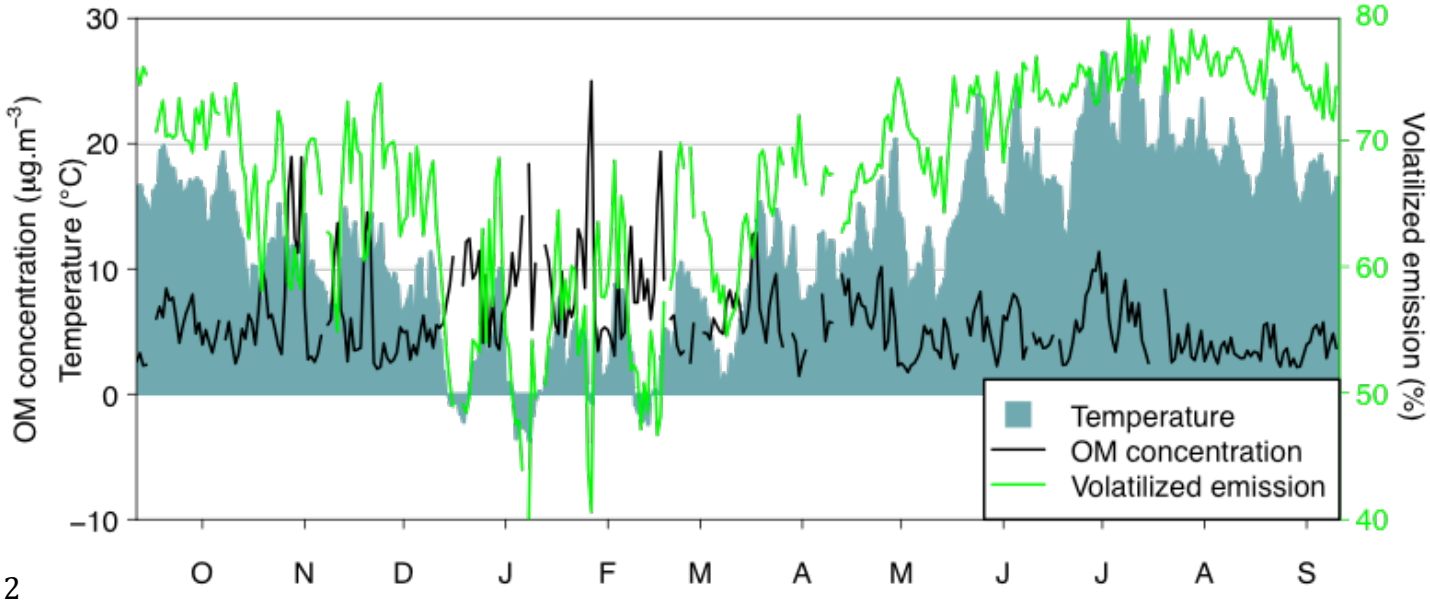

Figure S6: Volatilized POA emission fraction (green). Temperature at the MONTSOURIS station (in grey) and OM concentration at the PAR station (black) are also represented.

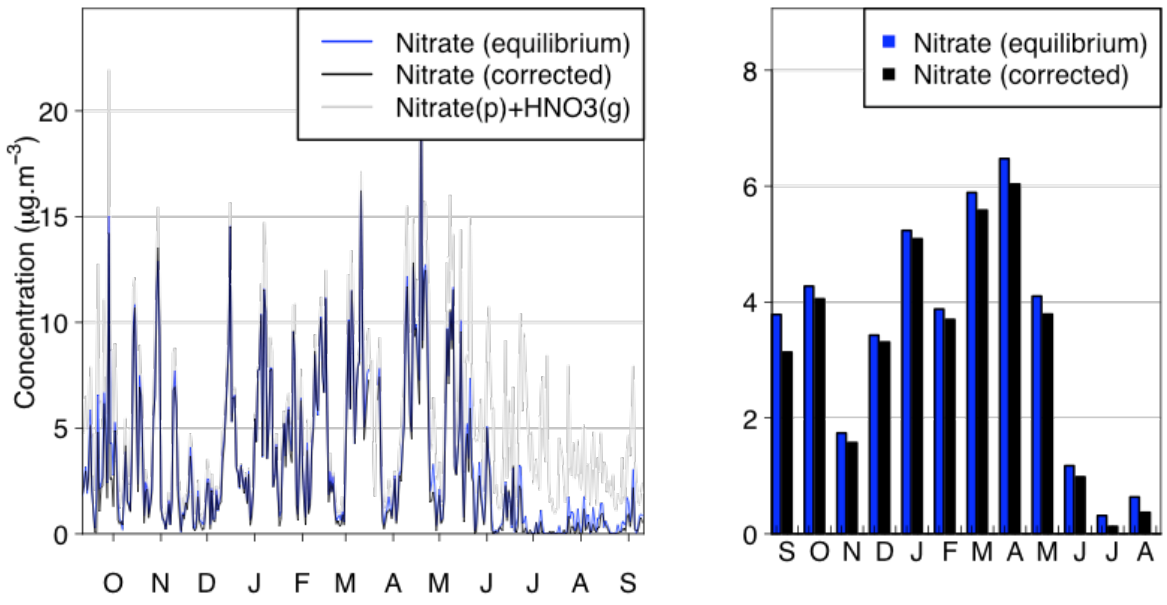

Figure S7: Daily (left panel) and monthly (right panel) particulate nitrate concentrations in Paris, taking into account the simulated (so-called *equilibrium*, blue line) and the observed (so-called *corrected*, black line) meteorology. The reservoir (particulate nitrate plus gaseous nitric acid) is represented in grey line.

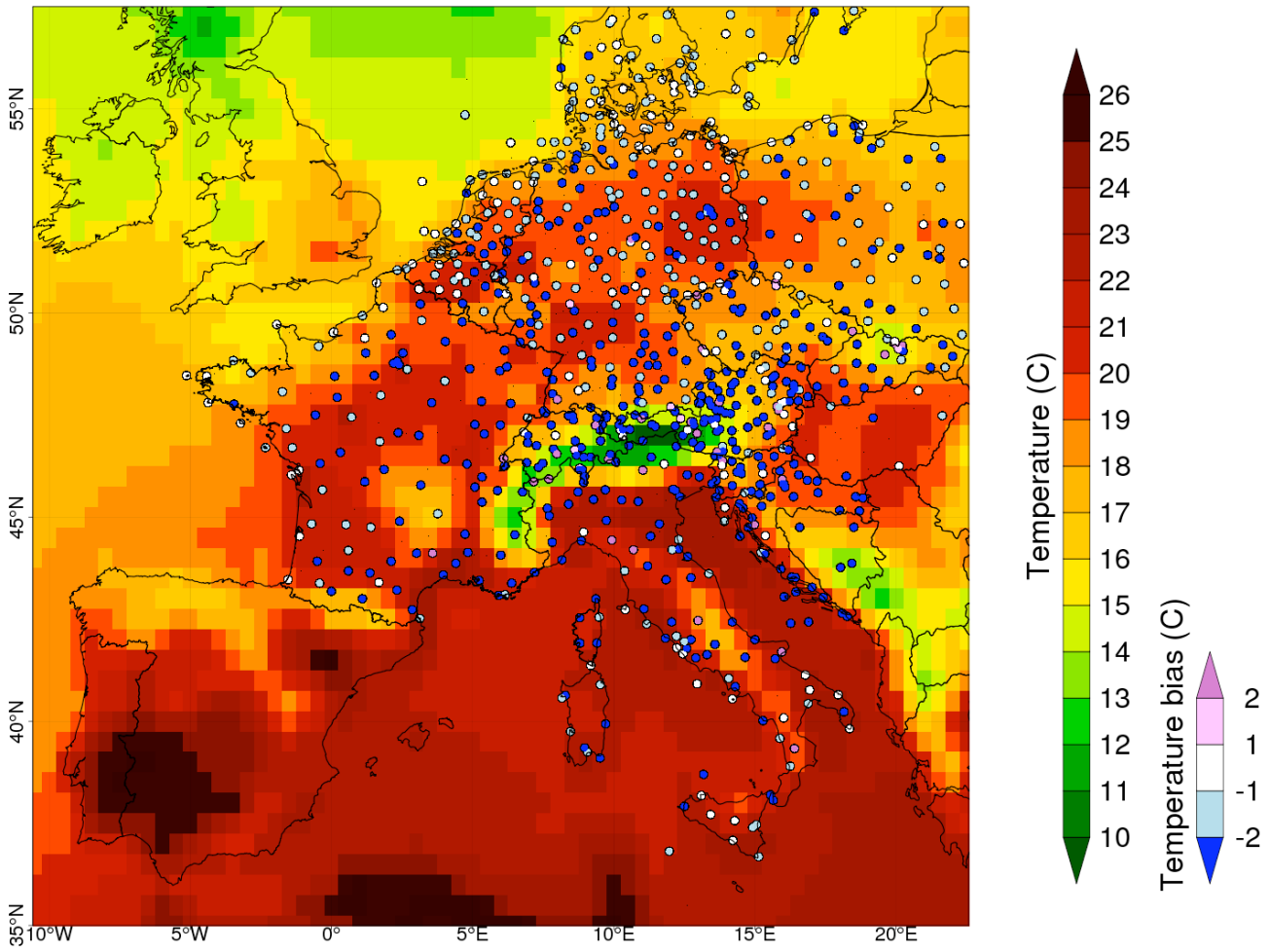

Figure S8: Simulated average temperature field over the period of 25 June – 5 July on the continental LAR domain, and mean temperature biases at BADC synoptic stations in a selection of countries.